A NOVEL STEP-UP MULTI-INPUT DC-DC CONVERTER FOR HYBRID ELECTRIC VEHICLES APPLICATION

DULIPUDI SUSMITA[1], CH. SABITHA[2]

[1]PG Scholar, Lingaya's Institute of Management and Technology, AP, India.

[2]Assistant Professor, Lingaya's Institute of Management and Technology, AP, India.

ABSTRACT

In this paper, a multi-input DC-DC converter is proposed and studied for hybrid electric vehicles (HEVs). Compared to conventional works, the output gain is enhanced. Fuel cell (FC), photovoltaic (PV) panel and energy storage system (ESS) are the input sources for proposed converter. The FC is considered as the main power supply and roof-top PV is employed to charge the battery, increase the efficiency and reduce fuel economy. The converter has the capability of providing the demanded power by load in absence of one or two resources.Moreover, power management strategy is described and applied in control method. A prototype of the converter is also implemented and tested to verify the analysis.

Keywords: Photovoltaic (PV), Fuel Cell (FC), Plug-In Hybrid Electric Vehicles (PHEVS), Hybrid Electric Vehicles (HEVS), Energy Storage System (ESS).

I. INTRODUCTION

Global warming and lack of fossil fuels are the main drawbacks of vehicles powered by oil or diesel. In order to overcome the aforementioned problems and regarding the potential of clean energies in producing electricity, car designers have shown interest in hybrid electric vehicles (HEVs) and plug-in hybrid electric vehicles (PHEVs). The overall structure of hybrid electric vehicle powered by renewable resources is depicted in Fig.1. Electric vehicles (EVs) have also been studied. EVs rely on energy stored in energy storage system (ESS). Limited driving range and long battery charging time are their main drawbacks. However, by using a bidirectional on/off board charger, they could have the V2G capability. Solar-assisted EVs have also been studied. Required location and size of PV panels have made them impractical at present. Employing fuel cell as the main power source of HEVs is the result of many years of research and development on HEVs. Pure water and heat are the only emissions of fuel cells. Furthermore, FCs have other advantages like high density output current ability, clean electricity generation, and high efficiency operation. However, high cost and poor transient performance are the main problems of FCs. It is important to note that vehicles mainly powered by FCs, are hybridized by ESSs. The main

advantages of hybridizing are enhancing fuel economy, providing a more flexible operating strategy, overcoming fuel cell cold-start and transient problems and reducing the cost per unit power.

A converter using coupled inductors is relatively better than isolation transformers since the coupled inductors have simpler winding structure and lower conduction loss [4]. However, the leakage inductors of the coupled inductors will consume significant energy for a large winding ratio. In such case, the voltage stress and the loss of the switches will both be increased. A boost converter with coupledinductor and active-clamp circuit is proposed in [4]. This boost converter can yield a high step-up voltage gain, reduce the voltage stress on switches, and recycle the energy in the leakage inductor.

II. PROPOSED TOPOLOGY

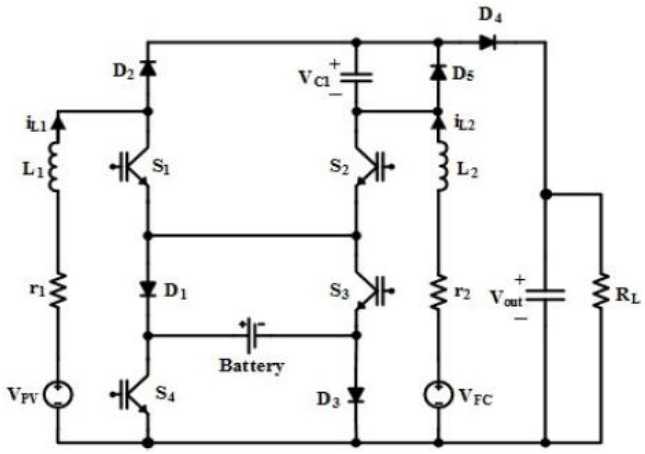

Fig. 1.Topology of the proposed converter

The structure of proposed three-input DC-DC boost converter is depicted in Fig. 2. The converter is formed of two conventional boost converters, substituting extra capacitor in one of the converters, and a battery to store the energy. Characteristic of the converter is suitable for hybrid systems. In this paper, behavior of the converter in terms of managing the sources is analyzed in power management and control part. Then *vPV* and *vFC* are two independent power sources, that output is based on characteristic of them. *L1*and *L2* are the inductances of input filters of PV panel and fuel cell. Using *L1* and *L2* as in series with input sources change PV and FC modules to current sources. *r1* and *r2* are *vPV*'s and *vFC*'s equivalent resistance, respectively. *RLoad* is the equivalent resistance of loads connected to the DC bus. *S1*, *S2*, *S3* and *S4* are power switches. Diodes *D1*, *D2*, *D3* and *D4* are used toestablish modes, which will be described. Capacitor *C1* is usedto increase output gain and output capacitor *Co* is performed as output voltage filter. System is operating in continuous conduct mode (CCM) to produce smooth current with least possible amount of current ripple.

The purpose of continuation load-flow is to find a continuum of load-flow solutions for a given load/generation change scenario, i.e. computation direction [Ibs96]. It is capable of solving the whole PV-curve. The singularity of continuation load-flow equations is not a problem; therefore the voltage collapse point can be solved. The continuation load-flow finds the solution path of a set of load-flow equations that are reformulated to include a continuation parameter [Ajj92]. This scalar equation represents phase conditions that guarantee the non-singularity of the set of equations. The method is based on prediction-correction technique. The prediction-correction technique applied to the PV-curve solution is illustrated in Figure 1. The intermediate results of the continuation process also provide valuable insight into the voltage stability of the system and the areas prone to voltage collapse.

III. MODELING OF CASE STUDY

PRINCIPLE OF OPERATION

In this section, principles of the proposed converter are discussed. Operation of the converter is divided into three states: 1- The load is supplied by PV and FC and battery is not used. 2- The load is supplied by PV, FC and battery, in this state battery is in discharging mode. 3- The load is supplied by PV and FC and battery is in charging mode.

TOPOLOGICAL MODES AND ANALYSIS:

I. First operation state (The load is supplied by PV andFC while battery is not used)

In this state, as it is illustrated in Fig. 2, there are three operation modes. During this state, the system is operating without battery charging or discharging. Therefore, there are two paths for current to flow (through *S3* and *D3* or*D1* and *S4*). In this paper *S3* and *D3* is considered as common path. However, *D1* and *S4* could be chosen as an alternative path. During this state, switch *S3* is permanently ON and switch *S4*is OFF.

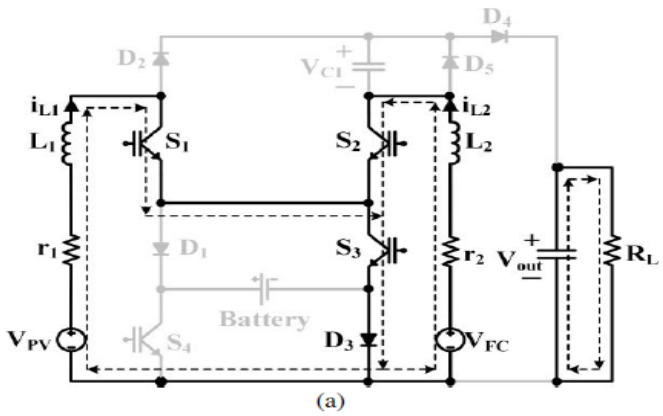

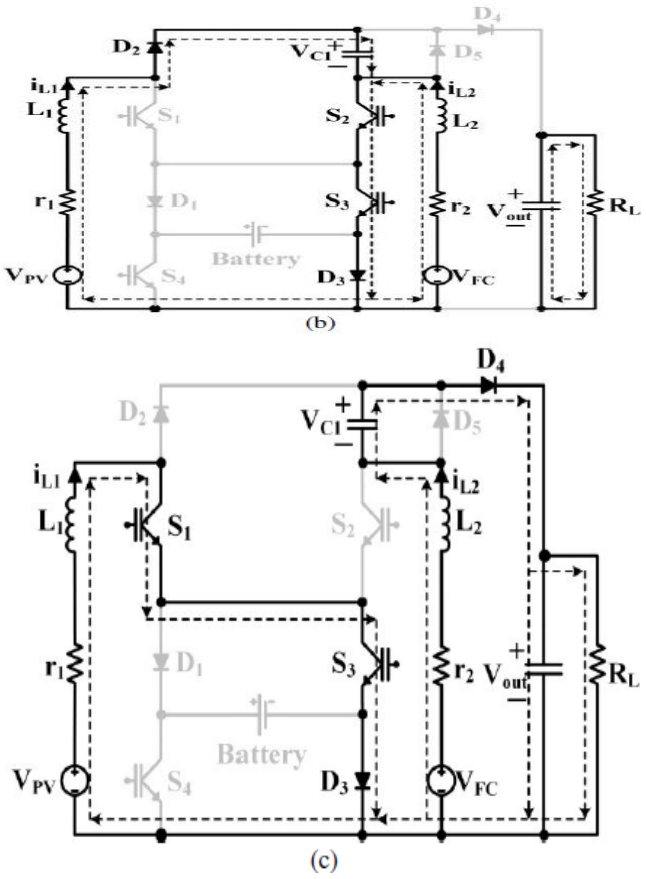

Fig. 2. Current-flow path of operating modes in first operating state. (a) Mode 1. (b) Mode 2. (c) Mode 3.

Mode 1 *(0< t <d1T):* In this interval, switches *S1*, *S2*, *S3* and diode *D3* are turned ON. Inductors *L1* and *L2* are charged via power sources *vPV* and *vFC*, respectively [see Fig. 2(a)].

Mode 2 (*d1T < t < d2T*)*:* In this interval, switch*S1* is turned OFF and *D2* is turned ON and *S2*, *S3* and *D3* are still ON. Inductor *L2* is still charged and inductor *L1* is being discharged via *vPV–vC1*[see Fig. 2(b)].

Mode 3 (*d2T < t < T):* In this interval, *S1* is turned ON and *S2* is turned OFF and *S3* and *D3* are still ON. Inductor *L1* is charged with *vPV* and inductor *L2* is discharged via *vPV+ vC1 –vo*[see Fig. 2(c)].

ISSN: 2250-3676
Volume-8, Issue-2, 326-336

II. Second operation state (The load is supplied by PV, FC and battery):

In this state, as it is illustrated in Fig. 4, there are four operation modes. During this state, the load is supplied by all input sources (PV, FC and battery). In first mode there is only one current path. However, in other three modes, there are two current paths (through S3 and D3 or D1 and S4). In this state, current flows through D1 and S4. Switch S4 is permanently ON during this state.

Mode 1 (0 < t < d1T): In this interval, S1, S2, S3and S4 are turned ON. InductorsL1 and L2 are charged by vPV + vBattery and vFC + vBattery respectively .

Mode 2 (d1T < t < d2T): In this interval, S1, S2, S4 and D1 are turned ON. InductorsL1 and L2 are charged by vPV and vFC respectively

Mode 3 (d2 T < t < d3T): In this interval, S2, S4, D1 and D2 are turned ON. Inductor L1 is discharged to capacitor C1 and L2 is charged by vFC

Mode 4 (d3T < t < d4T): In this interval, S1, S4, D1 and D4 are turned ON. Inductor L1 is charged by vPV and inductor L2 discharges C1 to the output capacitor.

III. Third operation state (The load is supplied by PV and FC while battery is in charging mode)

In this state, as it is illustrated in Fig. 3, there are four modes. During this state, PV and FC charges the battery and supply the energy of load. In the first and second operation modes, there are two possible current paths through *S3* and *D3* or *D1* and *S4*). The path *D1* and *S4* is chosen to flow the current in this state. During this state, switch *S3* is permanently OFF and diode *D1* conducts**.**

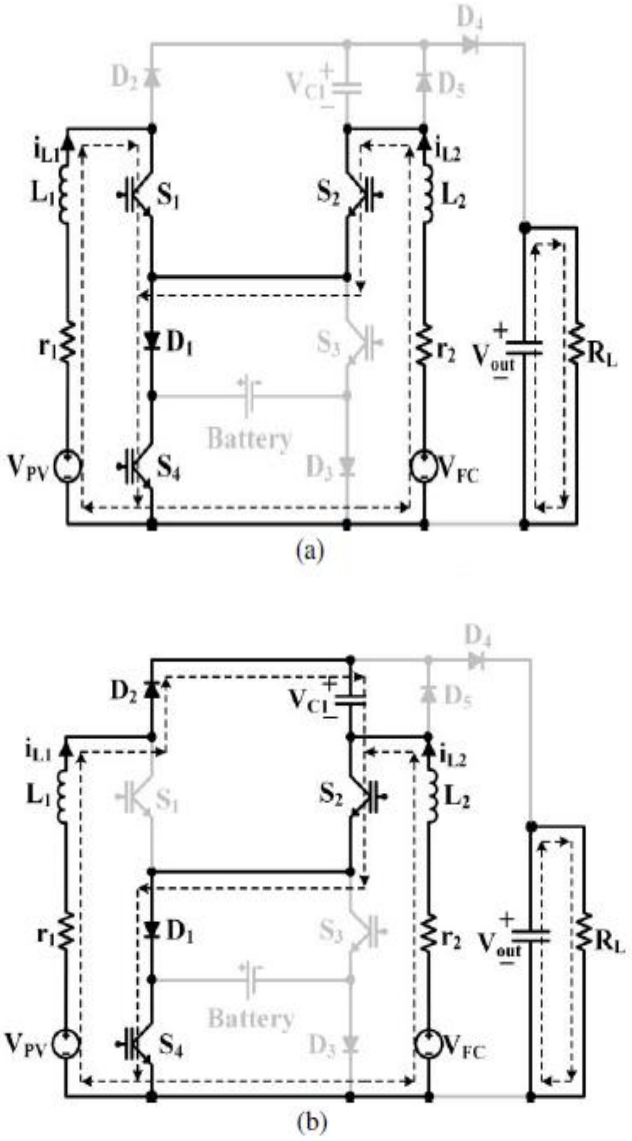

ISSN: 2250-3676
Volume-8, Issue-2, 326-336

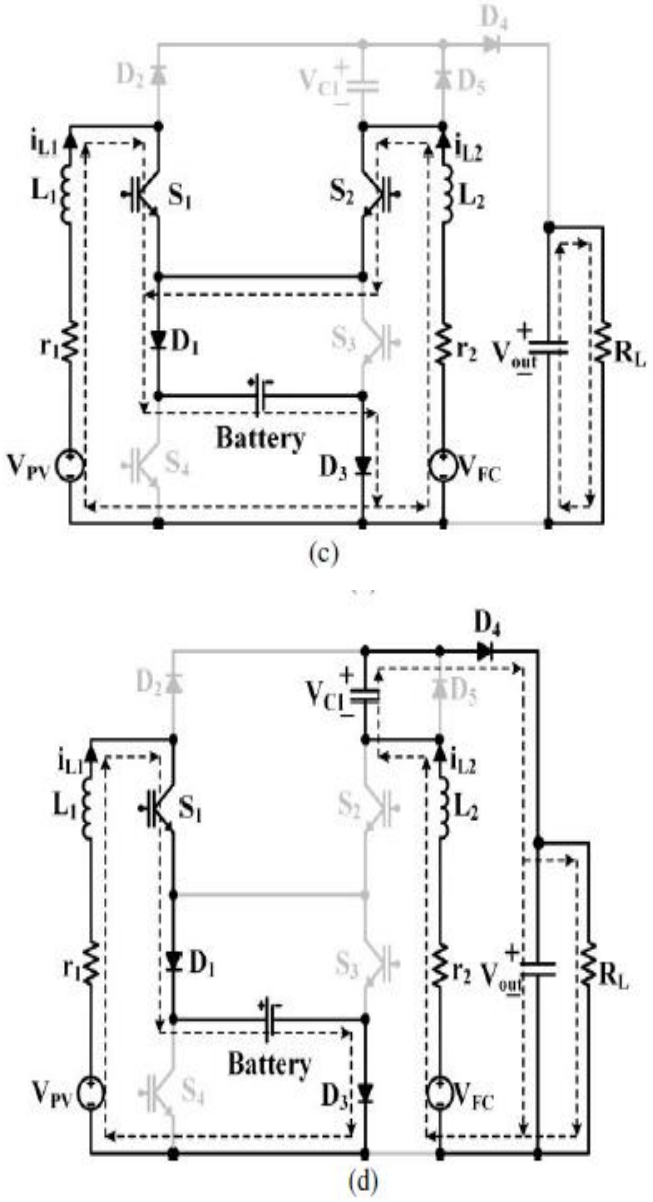

Fig. 3. Current-flow path of operating modes in third operating state. (a) Mode 1. (b) Mode 2. (c) Mode 3. (d) Mode 4.

Mode 1 *(0 < t < d1T):* In this interval, *S1*, *S2*, *S4* and *D1* are turned ON. Inductors *L1* and *L2* are charged by *vPV* and *vFC*,respectively [see Fig. 3(a)].

Mode 2 *(d1T < t < d2T):* In this interval, *S2*, *S4* and *D1* are turned ON. Inductor *L1*is discharged to capacitor *C1* and inductor *L2*ischarged by *vFC* [see Fig. 3(b)].

Mode 3 *(d2 T < t < d3 T):* In this interval, *S1*, *S2*, *D1* and *D3* are turned ON. Inductors *L1*and *L2* are charged by *vPV – vBattery* and *vFC – vBattery*, respectively [see Fig. 3(c)].

Mode 4 *(d3 T < t < d4 T):* In this interval, *S1*, *S4*, *D1* and *D4* are turned ON. Inductor *L1* is charged by *vPV - vBattery* and inductor *L2* is discharged by *vFC– vC1 – vo*[see Fig. 3(d)].

IV DYNAMIC MODELING AND CONTROL

Fig. 4 illustrates switching pattern for each state and each mode. To fulfill switching operation, a saw-tooth wave as a carrier is compared with signals *d1*, *d2*, *d3* and*d4*, which can independently control on state of power switches. Without considering output voltage utilized power of each sources PV, FC and battery can be controlled using *d1*, *d2*, *d3* and *d4*signals. The voltage gain of the proposed converter is compared with the converter proposed in [24] in fig. 7. As shown in this figure, the voltage gain of the proposed converter is higher than the converter proposed in [24]. Benefiting from high voltage gain, the proposed converter achieve the specific output voltage VO with less duty cycles in comparison with the converter proposed in [24] which increase the efficiency of the proposed converter. It is worth noting that in this figure, the inductor resistances are ignored and the voltage gain is compared in the first operation mode. Input voltages are also considered the same.

In order to control and analyze dynamic performance of the proposed converter, it should be modeled. As it has been mentioned, the presented converter operates in three states that first state is made of three modes and second and third states are contained of four modes. Each state operates to provide particular goals, which will be explained. In first state, output voltage and only one of the input power sources can be controlled.

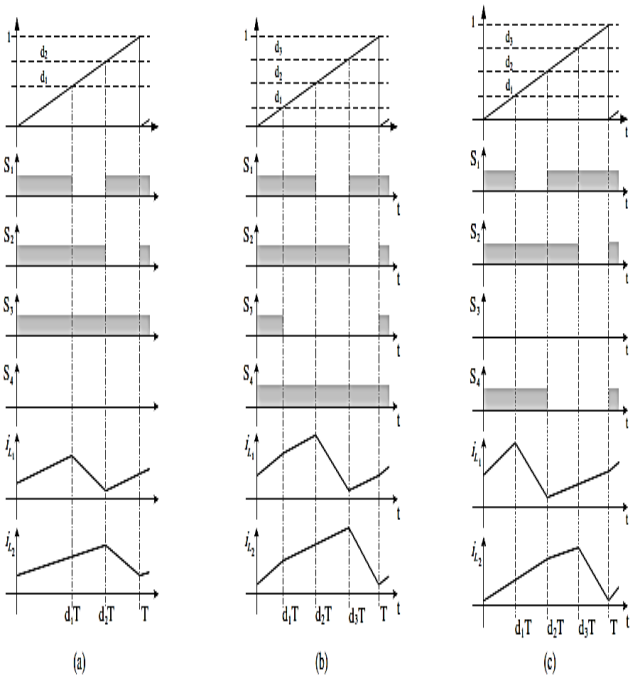

Fig. 4. Switching pattern for three states. (a) First state. (b) Second state. (c) Third state.

Due to this fact in this paper, we decide to control PV power source, which can be replaced by FC source as well. In second state because of interference the battery, output voltages and input sources power rate can be controlled. Third states' control parameters due to interference the battery is same as second state.

As mentioned previously interference the battery consists of two states, which in one of them battery will be charged and in one of them battery will be discharged. Selection of proper state (without battery, battery charging, battery discharging) is depends on power managing algorithm. Dynamic model of the proposed converter for each state is as follow: First state: In this state, *d1* and *d2*as control variables, control output voltage and power rate of one of the input sources that is consider PV in this paper.

$$L_1\frac{di_{L1}}{dt}=V_{PV}+(d_1-d_2)V_{C1}-r_1i_{L1} \quad (1)$$

$$L_2\frac{di_{L2}}{dt}=V_{FC}+(1-d_2)V_{C1}+(d_2-1)V_o-r_2i_{L2} \quad (2)$$

$$C_o\frac{dV_o}{dt}=(1-d_2)i_{L_2}-\frac{V_o}{R_{Load}} \quad (3)$$

$$C_1\frac{dV_{C1}}{dt}=(d_2-d_1)i_{L1}-(1-d_2)i_{L2} \quad (4)$$

Second state: In this state, three control variables d_1, d_2 and d_3 are used for controlling three state variables. In this state, state-space model of converter is:

$$L_1\frac{di_{L1}}{dt}=V_{PV}+d_1V_{bat}+(d_2-d_3)V_{C1}-r_1i_{L1} \quad (5)$$

$$L_2\frac{di_{L2}}{dt}=V_{FC}+d_1V_{bat}+(1-d_3)V_{C1}+(d_3-1)V_o-r_2i_{L2} \quad (6)$$

$$C_o\frac{dV_o}{dt}=(1-d_3)i_{L_2}-\frac{V_o}{R_{Load}} \quad (7)$$

$$C_1\frac{dV_{C1}}{dt}=(d_3-d_2)i_{L1}-(1-d_3)i_{L2} \quad (8)$$

Third state: In this state, same as second state, three state variables are controlled by three control variables d_1, d_2 and d_3, controlling. State-space model of converter in this state can be written as follows:

$$L_1\frac{di_{L1}}{dt}=V_{PV}+(d_2-1)V_{bat}+(d_1-d_2)V_{C1}-r_1i_{L1} \quad (9)$$

$$L_2\frac{di_{L2}}{dt}=V_{FC}+(d_2-d_3)V_{bat}+(1-d_3)V_{C1}+(d_3-1)V_o-r_2i_{L2} \quad (10)$$

$$C_o\frac{dV_o}{dt}=(1-d_3)i_{L_2}-\frac{V_o}{R_{Load}} \quad (11)$$

$$C_1\frac{dV_{C1}}{dt}=(d_2-d_1)i_{L1}-(1-d_3)i_{L2} \quad (12)$$

Assuming small signal method [25], input voltage, state variables and duty ratios consist of two parts: steady values $(\bar{V},\bar{X},\bar{D})$ and perturbations $(\tilde{v},\tilde{x},\tilde{d})$ that are:

$$v=\bar{V}+\tilde{v},\ x=\bar{X}+\tilde{x},\ d=\bar{D}+\tilde{d} \quad (13)$$

$$A=\begin{bmatrix} -r_1 & 0 & 0 & \bar{d}_1-\bar{d}_2 \\ 0 & -r_2 & \bar{d}_2-1 & 1-\bar{d}_2 \\ 0 & 1-\bar{d}_2 & -\frac{1}{R_{Load}} & 0 \\ \bar{d}_2-\bar{d}_1 & \bar{d}_2-1 & 0 & 0 \end{bmatrix},B=\begin{bmatrix} \bar{V}_{C1} & -\bar{V}_{C1} \\ 0 & \bar{V}_o-\bar{V}_{C1} \\ 0 & -\bar{i}_{L2} \\ -\bar{i}_{L1} & \bar{i}_{L1}+\bar{i}_{L2} \end{bmatrix}$$

$$C=\begin{bmatrix} 1&0&0&0 \\ 0&0&0&0 \\ 0&0&1&0 \\ 0&0&0&0 \end{bmatrix},\tilde{x}=\begin{bmatrix} \tilde{i}_{L1} \\ \tilde{i}_{L2} \\ \tilde{V}_o \\ \tilde{V}_{C1} \end{bmatrix},\tilde{u}=\begin{bmatrix} \tilde{d}_1 \\ \tilde{d}_2 \end{bmatrix} \quad (14)$$

Second state:

As mentioned, the first state comprises two control variables as well second and third states consist of three control variables. Due to aforementioned facts, the rank of transfer function matrix represents the number of control variables.

$$G^*_{2\times2} = \begin{bmatrix} 1 & -\frac{g_{12}}{g_{11}} \\ -\frac{g_{21}}{g_{22}} & 1 \end{bmatrix}$$

$$G_{3\times3}{}^* = \begin{bmatrix} 1 & \frac{g_{12}\cdot g_{32}-g_{12}\cdot g_{33}}{g_{11}\cdot g_{33}-g_{13}\cdot g_{31}} & \frac{g_{12}\cdot g_{23}-g_{13}\cdot g_{22}}{g_{11}\cdot g_{22}-g_{12}\cdot g_{21}} \\ \frac{g_{23}\cdot g_{31}-g_{21}\cdot g_{33}}{g_{22}\cdot g_{33}-g_{23}\cdot g_{32}} & 1 & \frac{g_{13}\cdot g_{21}-g_{11}\cdot g_{23}}{g_{11}\cdot g_{22}-g_{12}\cdot g_{21}} \\ \frac{g_{21}\cdot g_{32}-g_{22}\cdot g_{31}}{g_{22}\cdot g_{33}-g_{23}\cdot g_{32}} & \frac{g_{12}\cdot g_{31}-g_{11}\cdot g_{32}}{g_{11}\cdot g_{33}-g_{13}\cdot g_{31}} & 1 \end{bmatrix}$$

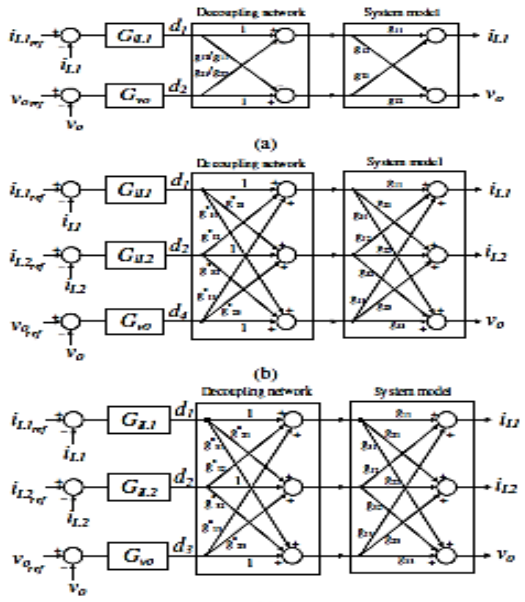

Fig. 5. Decoupling network for three states. (a) First state. (b) Second state.(b) Third state.

Where *y* and *u* are the output and input vectors,respectively, and *gij* is transfer function between *yi* and *uj*. In order to control proposed converter's desired state variables independently, decoupling the transfer function is needed [24]. Fig. 8 represent decoupling network for three operation states. Considering Decoupling Network *G** [24], [25] and *x=Gu**that *u** is the modified input consist of duty ratios *u*=G*u*. As a result, *x=GG*u*. Base on modern control theory [2], to provide each output of the matrixes be determined by each singular input, the matrix should be in diagonal arrange. Decoupling matrix *G*=G-1xu-1* for two controls and three control variables are given as above.

V POWER MANAGEMENT AND MPPT ALGORITHM

The multi-powered hybrid electric vehicle has aconstruction as depicted in Fig.1. In the drive system, the FC isthe main power supply. Roof-top PV panel is employed to reduce the fuel consumption and charging the battery. The battery is utilized as storage device. With a proper design, there will be no need for an external electrical supply to charge the battery [26]. The battery can be charged via PV, FC. In order to have the system operated in optimum region, the following criteria have to be ensured:

1. Electrical motor always supplies the demand power.
2. PV panel and FC operate in their optimal region.
3. The battery energy level should be always within the optimum region.

The power management procedure is described below and the flow chart of the strategy is depicted in Fig. 12.

I. Control signals, acceleration and brake, identify thecommand power.

II. In case command power is less than maximum PV power and battery energy level is less than minimum energy level, PV will work at MPP and extra energy will be stored in battery. If command power is less than maximum PV power but battery energy level is more than minimum energy level, PV will generate the command power and the battery remains off. In both conditions, FC is off.

III. If command power is more than maximum PV power, PV panel will operate in MPP and new command power will be defined.

IV. New command power is compared with FC's rated power. Given that the new command power is greater than rated power of FC, the FC will works at its rated power and battery will provide the rest of demanded power.

V. In next step, if new command power is less than minimum power of the FC and battery energy level is less than minimum energy level, the FC will work at its rated power and extra energy will be stored in battery.

VI. If new command power is less than minimum power of the FC but battery energy level is greater than minimum energy level, the FC will be turned off and the battery will provide the demanded power.

VII. If new command power is greater than minimum powerof the FC and battery energy level is greater than maximum energy level, the FC will provide the demanded power and the battery will be turned off.

VIII. If new command power is greater than minimum power of the FC but battery energy level is greater than maximum energy level, the FC will work at its rated power and extra energy will be stored in battery. Different MPPT methods including perturb and observe (P&O) algorithm [27], incremental conductance algorithm [28] and slide control [29] have been studied and presented in recent reports. Simple programming and low computation have made the P&O method a practical and widely used scheme among other schemes.

VI ADDITIONAL ADVANTAGES OF THECONVERTER, MAKING IT SUITABLE FOR HEVS

The proposed converter has the advantage of utilizingonly one resource in case the other power sources can't provide energy. This capability enhances the safety and reliability of the proposed converter.

Different possible states are described as follow:

PV ON and FC OFF:

Due to the long start-up time of fuel cell, this state happens mostly at the starting the car or when the car is run out of fuel cell gas. In this state, battery can becharged or discharged by PV. Because of the facts that FCis the main power supply and energy storage system (ESS) has a limited capacity, this state cannot be so long. In order to let the PV operate individually, switch *S2* is turned off and instead of capacitor *C1*, the power of PV is transferred to the output capacitor *Co*. According to the presented topology, battery can be charged and discharged via PV and by controlling switches*S1*, *S3* and *S4*.

PV OFF and FC ON:

As mentioned above, FC is the main power source to provides the demanded power by HEV individually because the energy of PV is less than FC and depends on climate situation. Therefore, an extra diode (*D5*) is paralleled with capacitor *C1*. The diode *D5* is off when capacitor *C1* is charged. When the FC is utilized individually, the capacitor *C1*discharges until its voltage is zero. When the voltage across capacitor *C1* is going to be negative, diode *D5*will be turned on
and clamps the voltage of capacitor *C1*.

VII SIMULATION RESULTS

PROPOSED CIRCUIT:

ISSN: 2250-3676
Volume-8, Issue-2, 326-336

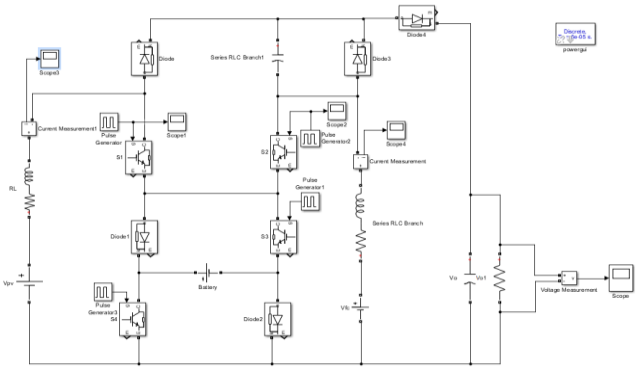

Fig. 6 Matlab Simulink for proposed converter

Here the Input given to the circuit is 100V DC and and the multiple outputs got as 150V and 300VDC.

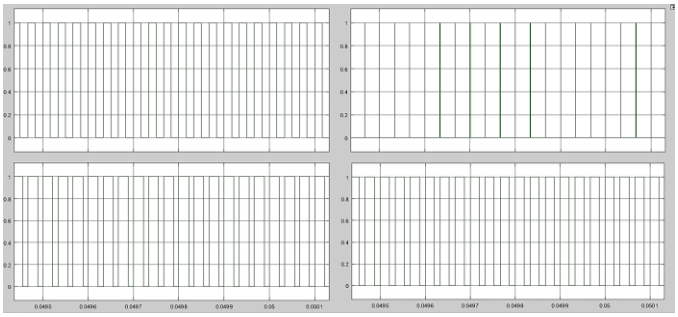

Fig .7 Pulses for the desired switches

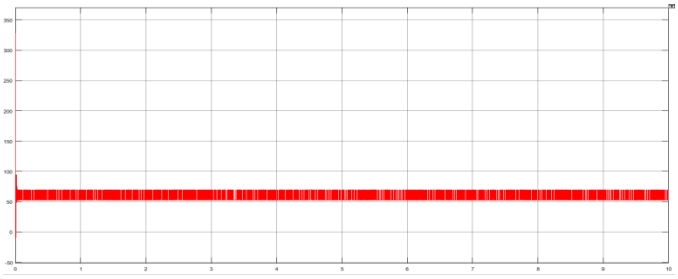

Fig. 8 Current across Indictor

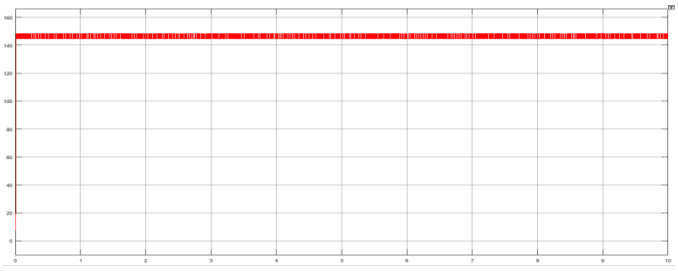

Fig.9 Current across Fuel cell

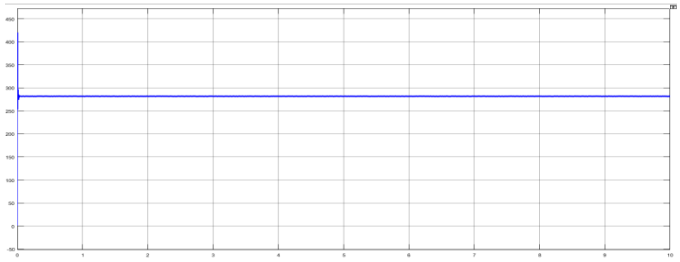

Fig .10 Output voltage Graph

VIII FUTURE SCOPE

In this paper, a novel three-input DC/DC converter isproposed and analyzed thoroughly. The converter has the capability of providing the demanded power by load in absence of one or two resources. The promising performance of the converter and employed control method offer a high reliability for utilizing the converter in industrial and domestic applications. The converter is modeled for three different operational states and utilized to design a proper controller. MPPT algorithm is achieved and along power management is utilized to apply the commands of controller. Meanwhile, employing power management and MPPT procedure will enhance the efficiency of the converter. Finally, a laboratoryprototype of the presented converted is implemented and results are taken and depicted. Results prove the analysis and performance of the converter.

IX REFERENCES

[1] A. Ostadi,and M. Kazerani.“Optimal Sizing of the BatteryUnit in a Plug-in Electric Vehicle,” *Vehicular Technology, IEEE Transactions on*, vol.63, no.7, pp.3077-3084, Sept. 2014.

[2] P. Mulhall , S. M. Lukic , S. G. Wirashingha , Y.-J. Lee and A. Emadi "Solar-assisted electric auto rickshaw

threewheeler", *Vehicular Technology, IEEE Transactions on*, vol. 59, no. 5, pp.2298 -2307 2010.

[3] H. J. Chiu, and L. W. Lin. "A bidirectional dcdc converter for fuel cell electric vehicle driving system", *IEEE Trans. Power Electron.*, vol. 21, no. 4, pp.950 -958, 2006.

[4] T. Markel, M. Zolot, K. B. Wipke, and A. A. Pesaran. "Energy storage requirements for hybrid fuel cell vehicles",*Advanced Automotive Battery Conf. 2003*

[5] S. Miaosen."Z-source inverter design, analysis, and its application in fuel cell vehicles", Ph.D. dissertation, Michigan State Univ., East Lansing, USA, 2007.

[6] O. Hegazy, R. Barrero, J. Van Mierlo, P. Lataire, N. Omar and T. Coosemans. "An Advanced Power Electronics Interface for Electric Vehicles Applications,"*IEEE Trans.Power Electron.*, Vol. 28, No. 12, pp. 1-14, Dec. 2013.

[7] M. R. Feyzi, S. A. KH. Mozaffari Niapour, F. Nejabatkhah, S. Danyali, and A. Feizi, " Brushless DC motor drive based on multi-input DC boost converter supplemented hybrid PV/FC/Battery power system," IEEE CCECE, 2011.

[8] R. J. Wai, C. Y. Lin; B. H. Chen, "High-Efficiency DC–DC Converter With Two Input Power Sources," *IEEE Trans. Power Electron*, vol. 27, no. 4, pp. 1862,1875, Apr 2012.

[9] L. J. Chien, C. C. Chen, J. F. Chen, Y. P. Hsieh, "Novel Three-Port Converter With High-Voltage Gain," *IEEE Trans. Power Electron*, vol. 29, no. 9, pp. 4693,4703, Sept. 2014.

[10] R. B. Mohammad, H. Ardi, R. Alizadeh, A. Farakhor, "Non-isolated multi-input–single-output DC/DC converter for photovoltaic power generation systems," *IET PowerElectron.*, vol. 7, no. 11, pp. 2806–2816, June. 2014.

[11] L. W. Zhou, B. X. Zhu, and Q. M. Luo, "High step-up converter with capacity of multiple input," *IET Power Electron.*, vol. 5, no. 5, pp. 524–531, May. 2012.

[12] A. Ajami, H. Ardi, A. Farakhor , "A Novel High Step-up DC/DC converter Based on Integrating Coupled Inductor and Switched-Capacitor techniques for Renewable Energy Applications," IEEE Trans. Power Electron., vol. 30, no. 8, pp. 4255-4263, Aug. 2015.

[13] H. Ardi, R. R. Ahrabi, S. N. Ravandanegh, "Non-isolated bidirectional DC–DC converter analysis and implementation," *IET Power Electron.*, vol. 7, no. 12, pp. 3033–3044, June. 2014.

[14] Duan, R.Y., Lee, J.D, "High-efficiency bidirectional DC–DC converter with coupled inductor," *IET Power Electron.*, vol. 5, no. 1, pp. 115–123, June. 2012.

[15] S. Danyali, S.H. Hosseini, G.B. Gharehpetian, "New Extendable Single-Stage Multi-input DC–DC/AC Boost Converter*," IEEE Trans. Power Electron.,* vol. 29, no. 2, pp. 775–788, Feb, 2014.

[16] L. Wang, Z. Wang, H. Li, "Asymmetrical Duty Cycle Control and Decoupled Power Flow Design of a Three-port Bidirectional DC-DC Converter for Fuel Cell Vehicle Application," *IEEE Trans. Power Electron.*, vol. 27, no. 2, pp. 891-904. Feb, 2012.

[17] S. Falcones, R. Ayyanar, X. Mao, "A DC–DC Multiport-Converter-Based Solid-State Transformer Integrating Distributed Generation and Storage," *IEEE Trans. Power Electron.*, vol. 28, no. 5, pp. 2192-2203. May, 2013.

[18] Y. M. Chen, A. Q. Huang, and X. Yu, "A High Step-Up Three-Port DC-DC Converter for Stand-Alone PV/Battery

Power Systems," *IEEE Trans. Power Electron.*, vol. 28, no. 11, pp. 5049 - 5062, Nov. 2013.

[19] K. Gummi, M. Ferdowsi, "Double-Input DC–DC Power Electronic Converters for Electric-Drive Vehicles— Topology Exploration and Synthesis Using a Single-Pole Triple-Throw Switch," *IEEE Trans. Ind. Electron.*, vol. 57, no. 2, pp. 617-623, Feb. 2010.

[20] R.-J. Wai , S.-J. Jhung , J.-J. Liaw and Y.-R. Chang. "Intelligent optimal energy management system for hybrid power sources including fuel cell and battery," *IEEE Trans. Power Electron.*, vol. 28, no. 7, pp. 3231-3244, 2013.